AIChE

Production of Argon Free Oxygen by Adsorptive Air Separation on Ag-ETS-10

Meng Shi, Jihong Kim, James A. Sawada, Jade Lam, Somayeh Sarabadan, Tetyana M. Kuznicki, and Steven M. Kuznicki
Dept. of Chemical and Materials Engineering, University of Alberta, Edmonton, Alberta, Canada T6G 2V4

DOI 10.1002/aic.13879

The purification of different components of air, such as oxygen, nitrogen, and argon, is an important industrial process. Pressure swing adsorption (PSA) is surpassing the traditional cryogenic distillation for many air separation applications, because of its lower energy consumption. Unfortunately, the oxygen product purity in an industrial PSA process is typically limited to 95% due to the presence of argon which always shows the same adsorption equilibrium properties as oxygen on most molecular sieves. Recent work investigating the adsorption of nitrogen, oxygen and argon on the surface of silver-exchanged Engelhard Titanosilicate-10 (ETS-10), indicates that this molecular sieve is promising as an adsorbent capable of producing high-purity oxygen. High-purity oxygen (99.7+%) was generated using a bed of Ag-ETS-10 granules to separate air (78% N_2, 21% O_2, 1% Ar) at 25°C and 100 kPa, with an O_2 recovery rate greater than 30%. © 2012 American Institute of Chemical Engineers *AIChE J,* 59: 982–987, 2013
Keywords: pure oxygen, argon free, nitrogen, Ag-ETS-10, separation

Introduction

The purification of different gases in air, such as nitrogen, oxygen and argon, is an important industrial process. Applications such as welding and cutting processes, plasma chemistry and laboratory applications require oxygen purity greater than 99%. Cryogenic air separation technology has long been used for producing high-purity oxygen and nitrogen for industrial and medical applications,[1] and is currently the most efficient technology when very large quantities of gas are required. The energetics and complexity of cryogenic distillation plants do not lend themselves well to point-of-use or on-demand high-purity O_2 applications. PSA separation of O_2 is well suited to applications where intermittent, on-demand requirements cannot be met using bottled gas or liquid O_2 delivery. Current PSA systems cannot deliver greater than 95% O_2 due to limitations in conventional air separation adsorbents.

An air separation pressure swing adsorption (PSA) process uses zeolites as adsorbents, as they preferentially adsorb nitrogen to oxygen.[2] The recovery of O_2 depends strongly on the adsorbent selected. Zeolites A and X have been used commercially as adsorbents for air separation.[3–6] A number of studies have investigated the utilization of various zeolites such as zeolite 5A and zeolite 13X as adsorbents in PSA processes.[4,6] In all the cases, the oxygen product purity is limited to 95% due to the presence of argon which has almost identical adsorption equilibrium properties to oxygen.

Another option to separate Ar from O_2 is by nonequilibrium methods. Another type of adsorbent, carbon molecular sieves (CMS), with a kinetic selectivity of oxygen over argon has been investigated and employed for production of purified oxygen and argon.[7–11] Ba-RPZ-3, a titanosilicate molecular sieve, was found to favor oxygen based on the sieving properties of the adsorbent and the difference in size between O_2 molecules and Ar atoms.[12] A two-step experimental study was reported by Hayashi et al. where direct air feed using Ca-X zeolite was used in the first step, producing 95% oxygen and 5% argon, and CMS is used in the second step to remove argon.[13] In both these studies, the O_2 is generated as the low-pressure product and will require recompression, adding cost and complexity to the process.

Silver exchanged zeolites such as silver mordenite,[14] silver exchanged zeolite A,[15] silver exchanged zeolite X,[16] and silver exchanged Li-Na-LSX zeolite[17] have all been reported to show some degree of argon over oxygen selectivity. In 2003, Air Products and Chemicals, Inc., reported that a vacuum and pressure swing adsorption unit using Ag-Li-LSX adsorbent allows the production of 99% oxygen with a recovery of 15%.[18]

In 2008, Kuznicki's group demonstrated that silver exchanged ETS-10, a mixed coordination titanosilicate molecular sieve, has an adsorptive selectivity for argon over oxygen.[19] The selectivity reached 1.49 in Henry's region, and is the highest selectivity reported to date for a silver-exchanged sieve.

This article describes the adsorptive separation performance of Ag-ETS-10 for air at ambient conditions on Ag-ETS-10 using a laboratory-scale demonstration unit. An adapted chromatographic method was developed to improve the quantification of O_2 and Ar in the product stream. The

---

Correspondence concerning this article should be addressed to S. M. Kuznicki at steve.kuznicki@ualberta.ca.

separation factor, breakthrough and desorption profiles are reported.

Experimental

Sample preparation

Na-ETS-10 was synthesized using conventional hydrothermal synthesis.[20] Preparation involved thoroughly mixing 50 g of sodium silicate (28.8% SiO_2, 9.14% Na_2O, Fisher), 3.2 g of sodium hydroxide (>97% NaOH, Fisher), 3.8 g of KF (anhydrous, Fisher), 4 g of HCl (1 M), and 16.3 g of $TiCl_3$ solution (Fisher), stirring the mixture in a Waring blender for 1 h, and then transferring the reactants to a 125 mL sealed, Teflon-lined autoclave (PARR Instruments) and heating at 215°C for 64 h. The material was then thoroughly washed with deionized water, and dried in an oven at 100°C. The ETS-10 adsorbent was ion exchanged by adding 5 g of ETS-10 to 10 g of silver nitrate (Fisher, USP) in 50 g of deionized water. The mixture was heated to 80°C for 1 h. The silver exchanged material was filtered, washed with deionized water and the exchanged procedure was repeated two more times (for a total of three exchanges). The silver exchanged ETS-10 was dried at 80°C in air. This method results in essentially quantitative silver exchange and final silver loading in excess of 30% of the finished material.[19] Ag-ETS-10 materials were pelletized by mixing 6 g of the molecular sieve with 2.5 g of Ludox HS-40 colloidal silica (Aldrich). The mixture was homogenized using a mortar and pestle and compressed in a pellet press at 69 MPa for 3 min. The resulting cakes were crushed and sieved to obtain particles of the size between 0.84-2 mm. The pelletized, crushed and sieved materials were used in both gas chromatographic and column separation experiments.

Characterization

Inverse-phase gas chromatography (IGC) analysis was performed on a Varian 3800 gas chromatograph (GC) equipped with a thermal conductivity detector (TCD). Test adsorbents were packed into 254 mm copper columns with OD of 6.35 mm. The columns were filled with 4 g of pelletized adsorbent (sieved to a size between 0.28–0.84 mm), which was activated at 200°C for 10 h under a helium flow of 30 mL/min. Analysis gases (Ar, O_2, 50/50 mixture of O_2-Ar, and air) were introduced by 1 mL pulse injections into the column at 30°C.

Low-pressure adsorption isotherms (up to 100 kPa) for nitrogen, oxygen and argon on crystalline adsorbent powders were measured volumetrically at 25°C using an AUTOSORB-1-MP from Quantachrome Instruments (Boynton Beach, FL). No binders or diluents were added to the adsorbent samples. Samples were activated at 200°C for 10 h *in vacuo* (<0.05 Pa). Experimental isotherms were fitted to the Langmuir adsorption isotherm (Eq. 1)

$$\frac{q_i}{q_{i,m}} = \frac{b_i P_i}{1 + b_i P_i} \tag{1}$$

with the standard deviations (Eq. 2)

$$\sigma = \sqrt{\frac{\sum \left(n_{\text{exp}} - n_{\text{calc}}\right)^2}{N - 2}} \tag{2}$$

where q_i is the amount adsorbed on the solid, P_i represents the pressure in the gas phase, $q_{i,m}$ is the saturation or maximum adsorption capacity, and b_i is the Langmuir (equilibrium) constant. n_{exp} is the experimentally measured adsorption at pressure P, is n_{calc} the adsorption calculated from the Langmuir equation at the same pressure. N is the number of measured experimental points. The Henry's Law constants $K_i = q_{i,m}\ b_i$, for each component were used to calculate the limiting selectivity of A over B (α Eq. 3).

$$\alpha = \frac{K_A}{K_B} \tag{3}$$

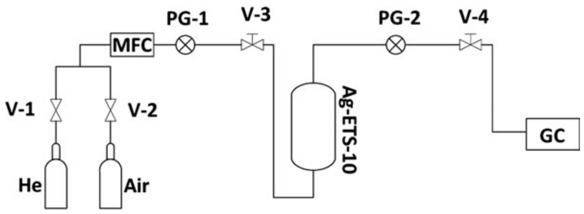

Figure 1. Schematic of one stage process for air separation on Ag-ETS-10.

Gas Chromatographic Separation and Determination of Argon and Oxygen in Air by Ag-ETS-10. Traditional chromatographic packings do not resolve the O_2 and Ar elution peaks very well and a significant amount of overlap between the two components is typical. This work aims to generate O_2 of purity greater than 99.5%, the quantification of minor amounts of Ar was necessary. A chromatographic method that enhances the resolution between the two elution peaks was developed for this work.

A Varian 3800 gas chromatograph (GC) equipped with a thermal conductivity detector (TCD) was adapted to operate at cryogenic temperatures. The method used Ag-ETS-10 granules packed into 508 mm copper columns having an OD of 6.35 mm. The columns were filled with 8 g of pelletized adsorbent (sieved to a size between 0.28–0.84 mm), which was activated at 200°C for 10 h under a helium flow of 30 mL/min. After activation, the 508 mm column was dipped in an ethanol and dry ice solution which maintains the column at a temperature close to −78°C. Analysis gases (Ar, O_2, 50/50 mixture of O_2-Ar, and 95/5 O_2-Ar) were introduced by 1 mL pulse injections into the column.

Laboratory-Scale Demonstration. Laboratory-scale demonstration is illustrated in Figure 1. Breakthrough experiments were performed using 130 g samples of pelletized, crushed, and sieved test adsorbents. The adsorbent was packed into a 150 mL cylindrical stainless steel chamber with an inner diameter of 20 mm and a length of 450 mm. The columns packed with adsorbent pellets were activated at 200°C for 10 h under 100 mL/min of helium flow.

The breakthrough experiments were run by conditioning the bed at 100 kPa with helium to purge any adsorbed gas from the system. The column temperature was maintained at 25°C using a water jacket around the bed coupled to a circulating water bath. Dry, compressed air was introduced into the fixed-bed column at a flow rate of 126 mL/min and the outlet gas composition was analyzed every 1.08 min using the adapted Varian 3800 gas chromatograph (GC) as described earlier. N_2 breakthrough was analyzed with the column at ambient condition, while the Ar and O_2 composition of the gas stream was analyzed at −78°C.

To analyze the solid-phase composition of the gas mixture, a desorption experiment was carried out on the bed. Figure 2 shows a schematic of the desorption experiment.

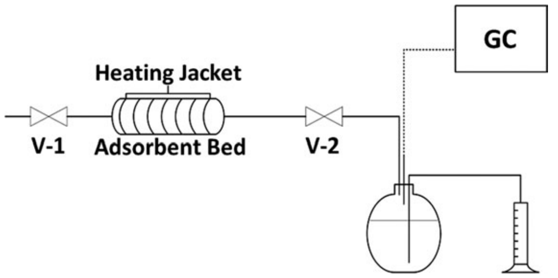

Figure 2. Schematic of desorption process.

After 40 min of adsorption, the system reaches equilibrium when the gas-phase outlet concentration is equal to the inlet gas concentration. GC analysis of the outlet composition was used to confirm that equilibrium was reached.

Once equilibrium is reached, the inlet of the bed is isolated and the bed is heated via a heating jacket until its internal temperature reaches 200°C. Heating the bed greatly reduces its adsorption capacity and forces the expanded gas downstream into the gas collector where it displaces a volume of water equal to the volume of collected outlet gas. Samples were taken from the outlet stream and analyzed by GC. After gas stopped flowing to the collector, the collected gas was sampled and analyzed by GC.

The gas collected includes both the adsorbed gas and the gas in the free space, but since the dead volume of the system is small compared to the amount of gas adsorbed, the collected gas should closely reflect the solid-phase composition of the bed.

Results and discussion

Figure 3 shows the results of IGC analysis of the separation of pure oxygen and argon, a mixture of 50–50% oxygen and argon, and air on Ag-ETS-10 at 25°C. The retention time for pure argon is larger than pure oxygen, indicating a preferred interaction between argon and Ag-ETS-10. This preference was also reflected in the analysis results for the 50–50% Ar—O_2 mixture. IGC analysis of the mixture shows that two peaks were present, and the greater degree of overlap between the O_2 and Ar peaks (compared to the pure components) suggests that the two species are competing for some of the same adsorption sites in the material. Similar to other reported silver-exchange sieves, Ag-ETS-10 has a strong affinity for N_2 which allows it to efficiently remove N_2 from an air stream. The IGC results demonstrate that Ag-ETS-10 can effectively separate the various components in air with a limiting selectivity (α) of 12.88 for N_2 over O_2, and of 1.41 for Ar over O_2.

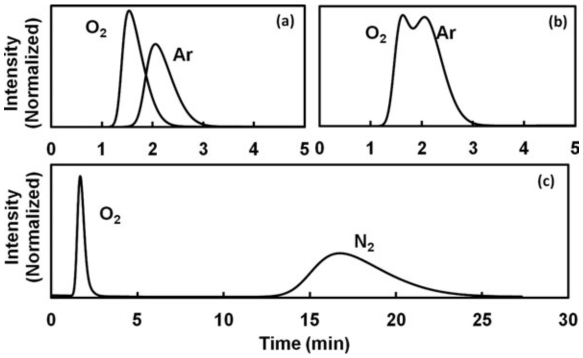

Figure 3. Typical gas chromatographic separations of N_2 over O_2, Ar over O_2 on Ag-ETS-10.

(a) Pure oxygen and argon (overlaid), (b) A 50–50% O_2-Ar mixture, and (c) air were injected into an Ag-ETS-10 column at 30°C using a 30 mL/min flow of helium carrier gas and their retention times were determined by IGC analysis.

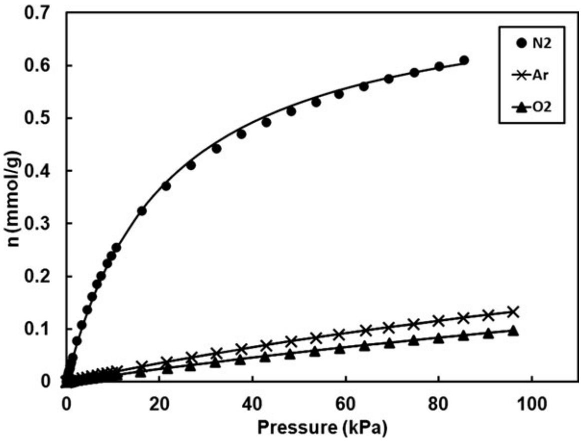

Figure 4. Equilibrium adsorption isotherms for N_2, Ar, O_2 on Ag-ETS-10 at 25°C. *P* is pressure, and *n* is capacity.

The selectivities of Ag-ETS-10 for N_2/O_2 and Ar/O_2 may also be calculated through the pure component adsorption isotherms; Figure 4 shows adsorption isotherms at 25°C in pressure range of 0-100 kPa for N_2, O_2 and Ar on Ag-ETS-10 together with the calculated Langmuir fits. The parameters of these Langmuir isotherms are listed in Table 1. Limiting selectivities of N_2 over O_2 (N_2 over Ar, Ar over O_2) at zero pressure can also be predicted by the Langmuir isotherms. These values are also presented in Table 1. The values calculated from the isotherm fits demonstrate that Ag-ETS-10 has a higher selectivity for argon over oxygen compared to other silver-exchanged sieves and has a strong preference for nitrogen over oxygen at zero pressure. The IGC and adsorption data are consistent in their estimation of adsorption selectivity and suggest that Ag-ETS-10, as a single adsorbent, can effectively and simultaneously remove N_2 and Ar from an air stream.

Figure 5 shows the results of GC analysis of the separation of pure oxygen and argon, a mixture of 50–50% oxygen and argon, and of 95–5% O_2-Ar on Ag-ETS-10 at −78°C. It demonstrates that the modified GC can quantitatively analyze an Ar/O_2 mixture which contains low levels of argon. Figure 6 shows a plot of a mixture that is 99.7% O_2 with 0.3% Ar. It can be seen in the plot that the Ar peak remains well-resolved even at this level of purity. From this result, we estimate our detection threshold for Ar to be approximately 0.1%, and, thus, our Ar-free oxygen has a purity of better than 99.9%.

Figure 7 depicts a breakthrough curve for air on Ag-ETS-10 at 25°C and 100 kPa which is represented in Table 2 as

Table 1. Langmuir Parameters for Adsorption Data in the Range of 0–100 kPa at 25°C

	Langmuir isotherm parameters			
Adsorbate	$q_{i,m}$ (mmol g^{-1})	b_i (kPa^{-1})	K_i (mmol kPa^{-1} g^{-1})	Selectivity
N_2	0.7545	0.0471	0.0355	$\alpha(N_2/O_2)=28$
Ar	0.4856	0.0039	0.0019	$\alpha(N_2/Ar)=18.7$
O_2	0.4844	0.0026	0.0013	$\alpha(Ar/O_2)=1.5$

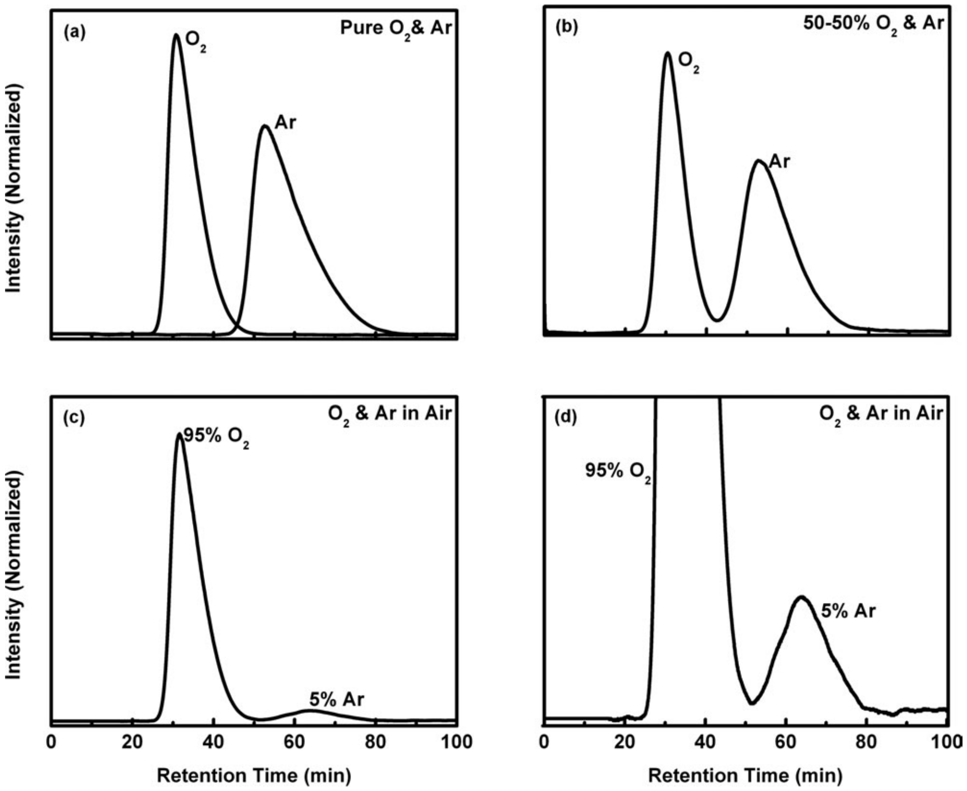

Figure 5. Gas chromatographic separation and determination of argon and oxygen in air by Ag-ETS-10.

(a) pure oxygen and argon, (b) 50–50% oxygen and argon, (c) 95–5% oxygen and Ar, and (d) magnified GC results for 95–5% oxygen and argon.

outlet concentration vs. time. With a continuous flow of feed gas (78% N_2, 21% O_2 and 1% Ar) at 126 mL/min, an argon-free oxygen product was detected at 11.88 min. The bed continued to produce an oxygen stream with no detectable argon (<0.3% Ar) for 1 min, after which point an argon concentration of 0.3% was detected. At 16.20 min, the nitrogen front started to break through. After 40 min of continuous flow in total, the concentration of N_2, O_2, and Ar in the outlet gas begins to reflect the inlet (feed gas) composition, indicating that the Ag-ETS-10 adsorbent has reached saturation.

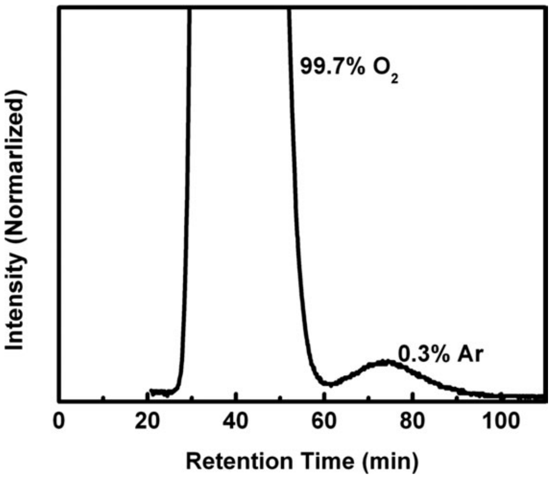

Figure 6. Gas chromatographic determination of 0.3% argon and 99.7% oxygen in air by Ag-ETS-10 (enlarged GC results).

Figure 8 shows the outlet gas flow rate monitored by an Agilent ADM 1000. The Agilent flow meter was calibrated using a Bronkhorst mini CORI—FLOW™ to allow the measured volumetric flow rates to be accurately converted to standard conditions. The outlet flow profile showed helium being displaced from the bed until a stream of high-purity O_2 was detected at 11.88 min. The Ar and N_2 fronts

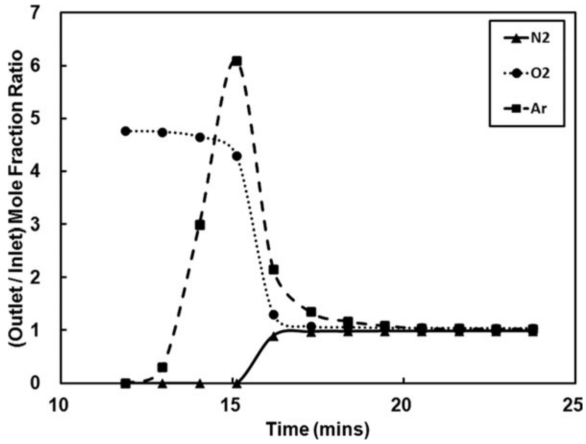

Figure 7. Air breakthrough curve on Ag-ETS-10 at ambient conditions.

Compressed air (a mixture of 78% N_2, 21% O_2 and 1% Ar) was introduced into a column containing 130 g of pelletized Ag-ETS-10 (sieved to a size between 0.28–0.84 mm) at a flow rate of 126 mL/min (bed volume 150 mL). Composition of the outlet gas was determined by GC analysis.

Table 2. Outlet Composition of the Breakthrough for N_2, O_2 and Ar

	Outlet Concentration(%)		
Time (min)	N_2	O_2	Ar
Feed in	**78.08**	**20.95**	**0.97**
0∼10.80	0.00	0.00	0.00
11.88	0.00	100.00	0.00
12.96	0.00	99.70	0.30
14.04	0.00	97.00	3.00
15.12	0.00	93.90	6.10
16.20	73.75	24.10	2.15
17.28	76.08	22.70	1.22
18.36	76.52	22.31	1.17
19.44	76.84	22.00	1.16
20.52	76.98	21.98	1.04
21.60	77.05	21.92	1.03
22.68	77.10	21.87	1.03
23.76	77.13	21.84	1.03
40	**77.96**	**21.05**	**0.99**

subsequently broke through at 12.96 min and 16 min, respectively. Integration of the flow profile between 0 min and 11.88 min yields a total volume of 381.5 mL of pure helium and this value is taken as the dead volume of the system. By integrating the measured flow between the O_2 and Ar breakthrough events, a quantity of 87.2 mL of 99.7+% O_2 is calculated. The breakthrough experiment was repeated 5 times with similar results each time.

The recovery rate for oxygen was calculated using the following equation (Eq. 4)

$$\text{Recovery rate of oxygen} = \frac{\text{volume of product} \times \text{oxygen composition}}{(\text{Feed in flow rate} \times \text{time} - \text{dead volume}) \times 21\%} \qquad (4)$$

given the feed flow rate of 126 mL/min, the dead volume of 381.5 mL, an average product flow of 88.5 ± 0.9 mL, and an average product purity of 99.7 ± 0.05%, the average recovery rate of oxygen over five cycles was 33.5%.

Based on the information collected, it should be possible to recover pure oxygen using a PSA containing Ag-ETS-10 as the sole adsorbent.

Thermal desorption was applied after 1 h of adsorption (a period sufficient to ensure that the system had reached equilibrium for all components). Figure 9 shows the outlet gas composition during the thermal desorption procedure and Table 3 lists the concentration values at the outlet during desorption. It was observed that the outlet gas composition was generally highly concentrated in N_2. At the end of the heating cycle, a total volume of 1200 mL of desorbed gas from the Ag-ETS-10 bed was collected. This desorbed gas should represent the gas adsorbed on the sieve. The average concentration for the total quantity of desorbed gas was 94% N_2 combined with a 6% of mixture of O_2 and Ar. The approximate N_2/O_2 selectivity for the bed can be estimated using the following equation (Eq. 5)

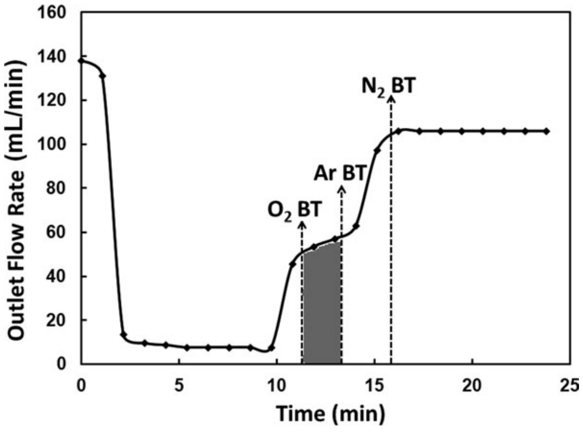

Figure 8. Product flow rate vs. time for the breakthrough of air over a bed of Ag-ETS-10.

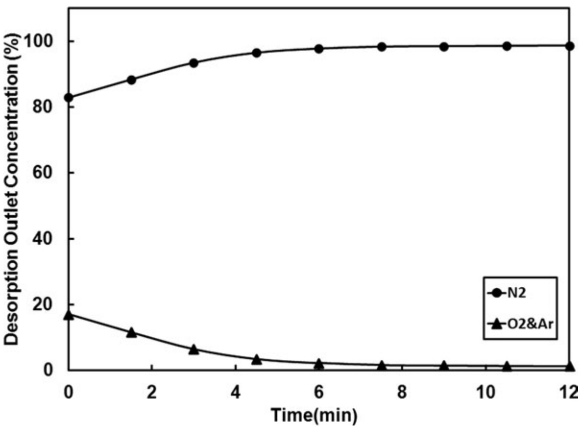

Figure 9. Outlet composition versus time during thermal desorption of the saturated Ag-ETS-10 bed.

$$S_{N2/O2} = \frac{X_{N_2} Y_{O_2}}{X_{O_2} Y_{N_2}} \qquad (5)$$

where X_{N2}, X_{O2} are the adsorbed phase concentration of N_2 and O_2, Y_{N2}, Y_{O2}, are the N_2 and O_2 concentration in air. Bed selectivity of N_2 over O_2 on Ag-ETS-10 at ambient conditions is 4.16.

The multicomponent breakthrough demonstration suggests that Ag-ETS-10 would be a very strong candidate as adsorbent for a PSA process to produce high-purity oxygen at ambient temperature.

Conclusions

Adsorption measurements demonstrate that Ag-ETS-10 is selective for argon over oxygen and nitrogen over oxygen. In this work, 87.2 mL of high-purity (99.7 + %) oxygen was produced over a 150 mL bed of Ag-ETS-10 granules using compressed air at 100 kPa and 25°C, with an O_2 recovery rate greater than 30. This suggests that Ag-ETS-10

Table 3. Outlet Composition of the Thermal Desorption of the Adsorbed Phase Gas

	Outlet Concentration (%)	
Time (min)	N_2	O_2 & Ar
0	82.95	17.05
1.5	88.43	11.57
3	93.52	6.48
4.5	96.52	3.48
6	97.77	2.23
7.5	98.36	1.64
9	98.5	1.5
10.5	98.61	1.39
12	98.7	1.30

could be an effective adsorbent in a PSA system designed for generating high purity O_2.

Acknowledgments

The authors thank Albana Zeko for assistance with manuscript development, Dr.Yadollah Maham, Omar Zarro, Tong Qiu, Lan Wu for their contributions. Support from the Natural Sciences and Engineering Research Council Industrial Research Chair in Molecular Sieve Separations Technology (S.M.K) is gratefully acknowledged, also thanks for the support from the Helmholtz-Alberta Initiative.

Literature Cited

1. Smith AR, Klosek J. A review of air separation technologies and their integration with energy conversion processes. *Fuel Process Technol*. 2001;70(2):115–134.
2. Yang RT.*Gas Separation by Adsorption Processes*. Boston: Butterworths; 1987.
3. Talu O, Li JM, Kumar R, Mathias PM, Moyer JD, Schork JM. Measurement and analysis of oxygen/nitrogen/5A-zeolite adsorption equilibria for air separation, *Gas Sep Purif*. 1996;10(3):149–159.
4. Moon I, Lee D, Yang J, Ryu H. Air separation by adsorption on molecular sieve 5A. *Kor J Chem Eng*. 1986;3(1):15–21.
5. Jee JG, Lee SJ, Moon HM, Lee CH. Adsorption dynamics of air on zeolite 13X and CMS beds for separation and purification. *J Int Adsorpt Soc*. 2005;11:415–420.
6. Zahra M, Jafar T, Masoud M. Study of a four-bed pressure swing adsorption for oxygen separation from air. *WASET*. 2008;47:99–103.
7. Reid CR, O'koye IP, Thomas KM. Adsorption of gases on carbon molecular sieves used for air separation. Spherical adsorptives as probes for kinetic selectivity. *Langmuir*. 1998;14(9):2415–2425.
8. Tan JS, Ani FN. Carbon molecular sieves produced from oil palm shell for air separation. *Sep Purif Technol*. 2004;35(1):47–54.
9. Jee J, Lee S, Lee C. Comparison of the adsorption dynamics of air on zeolite 5A and carbon molecular sieve beds. *Kor J Chem Eng*. 2004;21(6):1183–1192.
10. Rutherford SW, Coons JE. Adsorption equilibrium and transport kinetics for a range of probe gases in Takeda 3A carbon molecular sieve. *J Colloid Interface Sci*. 2005;284(2):432–439.
11. Jee JG, Kim MB, Lee CH. Pressure swing adsorption processes to purify oxygen using a carbon molecular sieve. *Chem Eng Sci*. 2005;60(3):869–882.
12. Anson A, Kuznicki SM, Kuznicki T, Dunn BC, Eyring EM, Hunter DB. Separation of argon and oxygen by adsorption on a titanosilicate molecular sieve. *Sep Sci Technol*. 2009;44(7):1604–1620.
13. Hayashi S, Kawai M, Kaneko T. Dynamics of high purity oxygen PSA. *Gas Sep Purif*. 1996;10(1):19–23.
14. Wilkerson BE. The Adsorption of Argon and Oxygen on Silver Mordenite [Master's thesis]. The Ohio State University; 1990.
15. Sebastian J, Jasra RV. Sorption of nitrogen, oxygen, and argon in silver-exchanged zeolites. *Ind Eng Chem Res*. 2005;44(21):8014–8024.
16. Chiang RL, Whitley RD, Ostroski JE, Dee DP. Argon/oxygen selective X-zeolite. US Patent 6432170B1. 2002.
17. Hutson ND, Rege SU, Yang RT. Mixed cation zeolites: LixAgy-X as a superior adsorbent for air separation. *AIChE J*. 1999;45(4):724–734.
18. Dee DP, Chiang RL, Miller EJ, Whitley RD. High purity oxygen production by pressure swing adsorption. US Patent 6544318B2. 2003.
19. Anson A, Kuznicki SM, Kuznicki T, Haastrup T, Wang Y, Lin CCH, Sawada JA, Eyring EM, Hunter D. Adsorption of argon, oxygen, and nitrogen on silver exchanged ETS-10 molecular sieve. *Microporous Mesoporous Mater*. 2008;109(1–3):577–580.
20. Kuznicki SM. Large-pored crystalline titanium molecular sieve zeolites. US Patent 4853202A. 1989.

Manuscript received Oct. 24, 2011, revision received Apr. 26, 2012, and final revision received Jun. 19, 2012.